Available online at www.sciencedirect.com
SCIENCE DIRECT®
Construction and Building Materials 20 (2006) 220–228
Construction and Building MATERIALS
www.elsevier.com/locate/conbuildmat

Pseudo-dynamic testing of unreinforced masonry building with flexible diaphragm and comparison with existing procedures

Jocelyn Paquette [a,*], Michel Bruneau [b]

[a] Heritage Conservation Directorate, Public Works and Government Services Canada, 25 Eddy, Gatineau, Que., Canada K1A 0M5
[b] Multi-Disciplinary Centre for Earthquake Engineering Research, Department of Civil and Environmental Engineering, 130 Ketter Hall, State University of New York, Buffalo, NY 14260, United States

Received 11 April 2005; received in revised form 11 April 2005; accepted 30 August 2005
Available online 17 October 2005

Abstract

A full-scale one-story unreinforced brick masonry specimen having a wood diaphragm was subjected to earthquake excitations using pseudo-dynamic testing. The specimen was designed to better understand the flexible-floor/rigid-wall interaction, the impact of wall continuity at the building corners and the effect of a relatively weak diaphragm on the expected seismic behavior. The unreinforced masonry walls of this building were also repaired with fiberglass materials and re-tested. The overall building was found to be relatively resilient to earthquake excitation, even though cracking was extensive. The repair procedure was demonstrated to enhance this behavior. It was found that even though the diaphragm did not experience significant inelastic deformation, some (but not all) of the existing seismic evaluation methodologies accurately capture the rocking/sliding behavior that developed in the shear walls under large displacement. The response of the wood diaphragm and its interaction with the shear walls have also been studied. The evaluation of experimental results and the comparison with the existing procedures have revealed that the diaphragm deflections observed experimentally closely matched those predicted using the FEMA 356 and ABK models.

Keywords: Unreinforced masonry; Wood diaphragm; Seismic response

1. Introduction

The Uniform Code for Building Conservation (UCBC) (ICBO [1]) *Seismic Strengthening Provisions for Unreinforced Masonry Bearing Wall Buildings* presents a systematic procedure for the evaluation and seismic strengthening of unreinforced masonry (URM) bearing wall buildings having flexible diaphragms. This special procedure, adapted from one developed by the ABK joint venture (ABK [2], FEMA [3]), used extensively in the Los Angeles area, and described in details by Bruneau [4,5], has made it economically possible to significantly reduce the seismic hazard posed by these buildings, as evidenced by the considerably lesser damage suffered by seismically retrofitted URM buildings in recent earthquakes, compared to non-retrofitted ones (Bruneau [6,7], Rutherford and Chekene [8]). However, even though this procedure is founded on extensive component testing, full scale testing of an entire URM building having wood diaphragms has not been conducted. Such a test would complement the computer simulations and small-scale shake table tests by other researchers (Costley and Abrams [9]).

2. URM specimen

The single-story full-scale unreinforced brick masonry building constructed for this experimental program is shown in Figs. 1–3. This rectangular shaped building was constructed with two wythes solid brick walls (collar joint filled) and type O mortar was used to replicate old con-

* Corresponding author. Fax: +819 953 7482.
E-mail addresses: Jocelyn.Paquette@pwgsc.gc.ca (J. Paquette), bruneau@acsu.buffalo.edu (M. Bruneau).

0950-0618/$ - see front matter © 2005 Elsevier Ltd. All rights reserved.
doi:10.1016/j.conbuildmat.2005.08.025

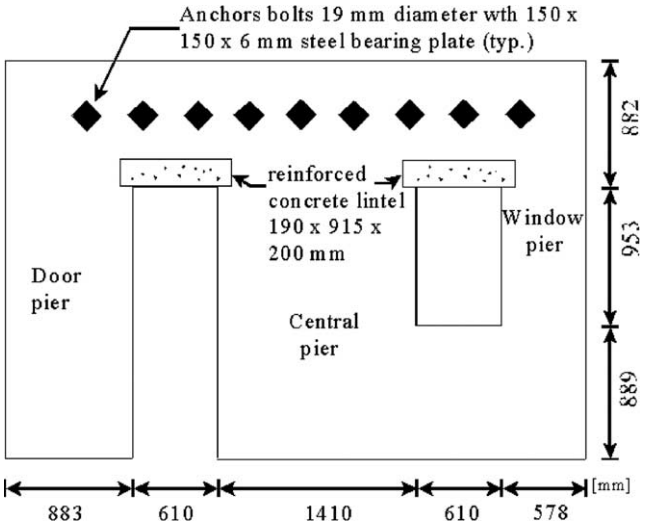

Fig. 1. Elevation of URM specimen (parallel to loading): east wall.

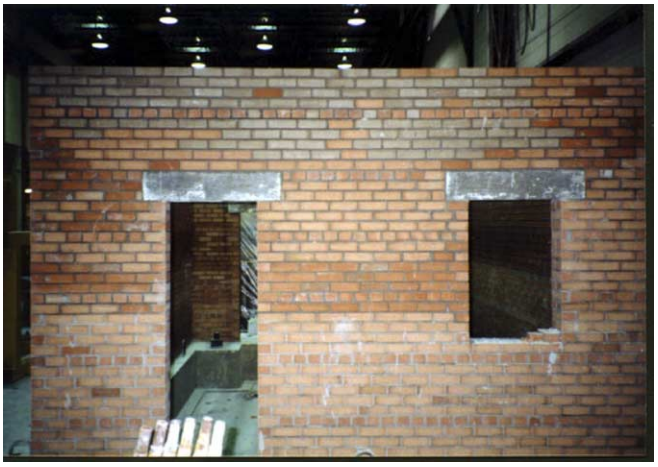

Fig. 2. URM specimen.

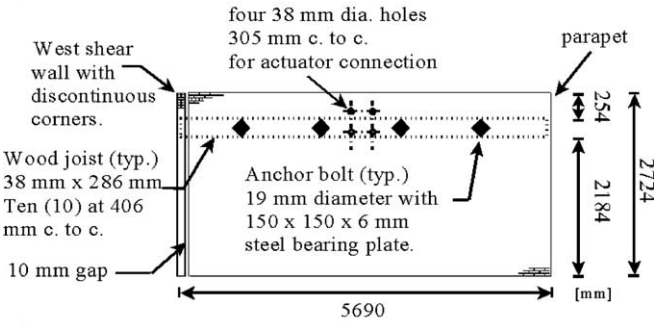

Fig. 3. Elevation of URM specimen (normal to loading): south wall.

struction methods and materials (URM built in North America before the 1960s). The specimen has two load-bearing shear walls, each with two openings (a window and a door). Shear walls were designed such that all piers would successively develop a pier-rocking behavior during seismic response. This rigid-body mechanism is recognized

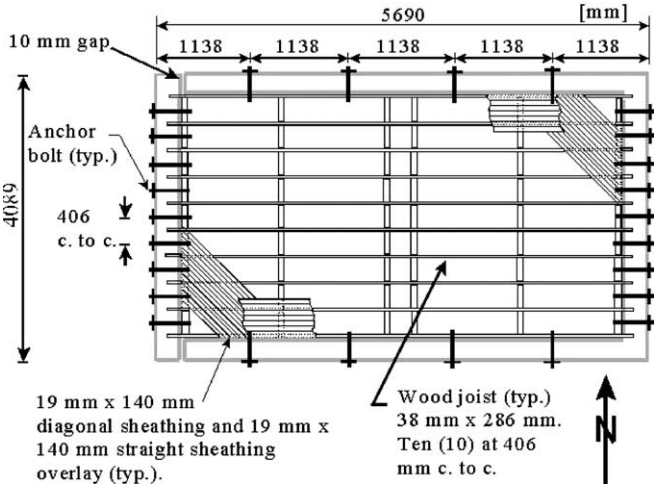

Fig. 4. Wood sheathed diaphragm framing details.

by the UCBC to be a stable failure mechanism. The specimen has a flexible diaphragm constructed with wood joists and covered with diagonal boards with a straight board overlay (Fig. 4). The diaphragm was anchored to the walls with through-wall bolts in accordance to the special procedure of the UCBC. A parapet was built above the wood joist, and an additional gravity load on the diaphragm was provided by plastic containers filled with water, simulating a 2.4 kPa live load. Material properties were obtained from simple component tests, such as a three-point flexural bending test of a small beam in order to determine the tensile strength of the mortar used.

At the corners of the building at one of its ends, gaps were left between the shear wall and its perpendicular walls. At the other end, walls were continuous over the building corners. This permits a comparison between the plane models considered by many engineers and the actual behavior at the building corners, and allows to assess the significance of this discrepancy on seismic performance, particularly when piers are expected to be subjected to rocking. To some extent, it also permits to observe the impact of in-plane rotation of the diaphragm's ends on wall corners.

2.1. Experimental procedure

The unreinforced brick masonry specimen was subjected to a first series of tests under an earthquake of progressively increasing intensity (Paquette and Bruneau [10]). The test set-up is shown in Fig. 5. Non-linear inelastic analyses were conducted to determine an appropriate seismic input motion that would initiate significant pier rocking from the diaphragm response. The selected input motion is a synthetic ground motion for La Malbaie, Canada with a peak ground acceleration of 0.453*g* (Fig. 6).

Figs. 7–9 illustrate the behavior observed during the tests. A stable combined rocking and sliding mechanisms formed and large deformations developed without significant strength degradation. The hysteretic response of the

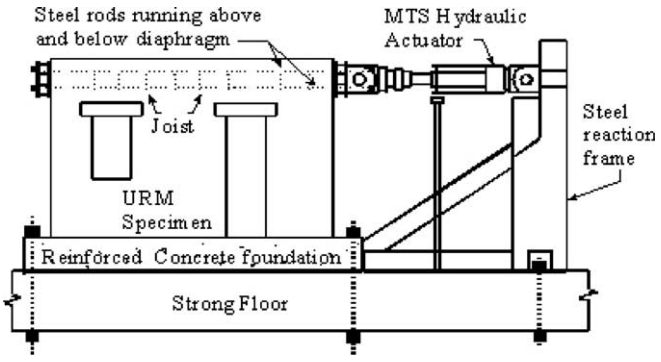

Fig. 5. Test setup.

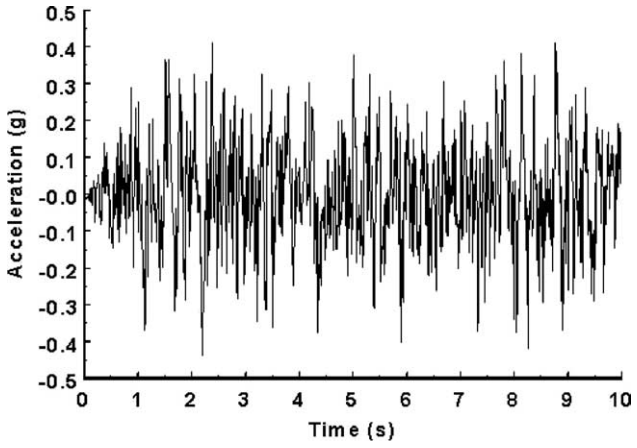

Fig. 6. Acceleration time history for La Malbaie (peak ground acceleration of 0.453*g*).

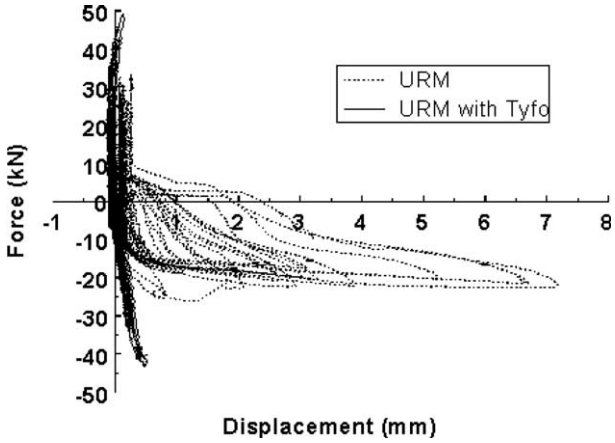

Fig. 8. Door pier rocking response before and after Tyfo repair for La Malbaie × 2.0.

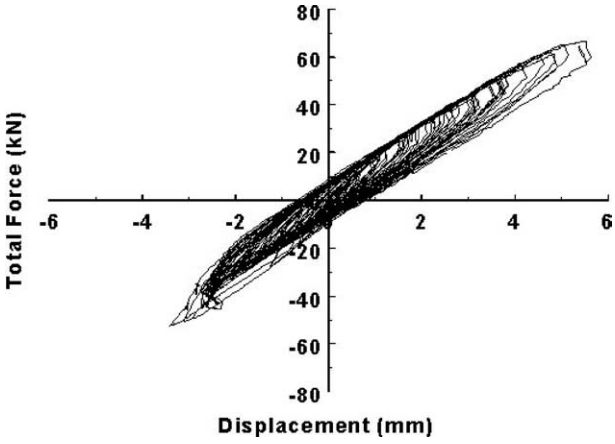

Fig. 9. Hysteretic response of wood diaphragm at center span during La Malbaie × 2.0.

west and east shear walls is shown in Fig. 7(a), and (b), respectively. Special clip gages were installed at expected crack location around all the piers to record crack opening and closing during the pier's rocking cycle. This rocking motion is clearly shown in Fig. 8 where the crack opens when the force acts in one direction and remains closed in the reverse direction. A different stiffness for the east and west walls was observed at the beginning, during low intensity seismic motion. However, the hysteretic curves during a higher intensity seismic motion, La Malbaie × 2.0, are very similar, as shown in Fig. 7(a) and (b). This suggests that the effect of continuous/discontinuous corners becomes somehow negligible during high intensity seismic motion.

These results are compared with predictions from existing seismic evaluation methodologies for URM such as the NEHRP Handbook for Seismic Evaluation of Existing

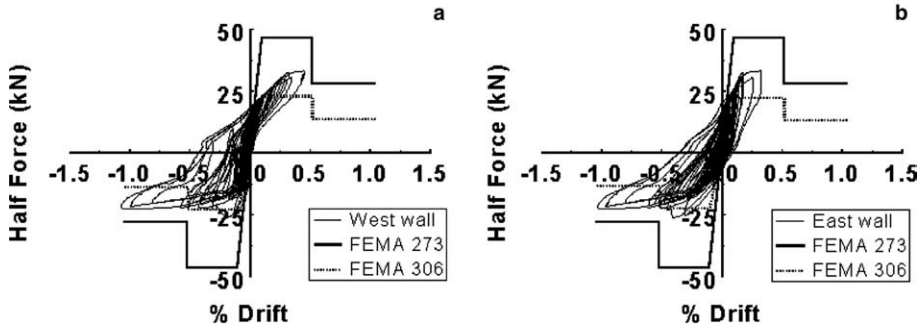

Fig. 7. Hysteretic response during La Malbaie × 2.0, and comparison with idealized force-deflection model using expected capacities from FEMA 273 and FEMA 306 for: (a) west wall and (b) east wall.

Buildings (FEMA 178) (FEMA [3]), Appendix 1 of the UCBC (ICBO [1]) (Appendix 1 of the UCBC is similar to the FEMA 178 document but is based on allowable stress values, i.e., working stress design), Appendix A of the Canadian Guidelines for Seismic Evaluation of Existing Buildings (CGSEEB) (NRC [11]) (Appendix A of the CGSEEB is also similar to FEMA 178 but is adjusted for Canadian codes and practice), the NEHRP Guidelines for the Seismic Rehabilitation of Buildings (FEMA 273) (FEMA [12]), and FEMA 306 (FEMA [13]) entitled Evaluation of Earthquake Damaged Concrete and Masonry Wall Buildings.

2.2. Evaluation procedure

The evaluation of URM walls subjected to lateral forces applied in-plane is performed by calculating the capacities corresponding to each possible individual modes of behavior, the lowest value being the governing failure mode. All behavior modes mentioned below, are summarized in Table 1, showing in which documents they are addressed.

The possible modes of behavior include: pier rocking (V_r), sliding shear resistance (V_a) (termed "bed joint sliding with bond plus friction" (V_{bjs1}) in FEMA 273 and FEMA 306), bed joint sliding with friction only (V_{bjs2}) (found only in FEMA 306), diagonal tension (V_{dt}), and toe crushing (V_{tc}). Note that both V_{dt} and V_{tc} are found only in FEMA 273 and FEMA 306. Both rocking and bed joint sliding are considered to be deformation-controlled behaviors able to sustain large lateral deformations while strength remains almost constant, while diagonal tension and toe crushing are considered as force-controlled behaviors.

Following the procedure outlined in FEMA 273, the governing failure mode for each pier is rocking (V_r), as shown in Table 2. Thus, the lateral capacity for each shear wall is the summation of each individual pier rocking capacity, and is equal to 46.7 kN. Likewise, FEMA 306 gives a procedure to evaluate lateral capacity based on observed damage caused by an earthquake. As such, it requires using the effective height (h_{eff}) of pier reflecting the observed crack pattern. Therefore, the capacities for the individual modes of behavior for each pier shown in Table 2, were re-calculated using the crack pattern observed after pseudo-dynamic tests. The effective height used and resulting capacities are presented in Table 3.

The FEMA 273 non-linear static procedure was used to establish the idealized non-linear force-deflection relation for the wall. In this procedure, permissible deformations are established as drift percentages for primary elements (walls considered to be part of the lateral-force system) and secondary elements (walls not considered as part of the lateral-force-resisting system but supporting gravity loads) for the different performance levels of immediate occupancy (IO), life safety (LS), and collapse prevention (CP). The expected capacities for FEMA 273 (46.7 kN), and FEMA 306 (23.0 and 22.2 kN for the west and east

Table 1
Possible lateral behavior modes as per different codes and methodologies

Modes of behavior	FEMA 178	CGSEEB	UCBC 1997	FEMA 273	FEMA 306
Rocking	X	X	X	X	X
Shear/bed joint sliding w/bond + friction	X	X	X	X	X
Bed joint sliding w/friction only					X
Diagonal tension				X	X
Toe crushing				X	X

Table 2
Calculation of pier possible behavior mode based on FEMA 273

Pier	Pier's height H (mm)	Rocking V_r (kN)	Bed-joint sliding V_{bjs1} (kN)	Diagonal tension V_{dt} (kN)	Toe crushing V_{tc} (kN)
Door	1842	6.08	39.8	24.5	6.70
Central	953	34.5	65.2	59.8	37.9
Window	953	6.11	27.0	16.6	6.72

Table 3
Calculation of pier possible behavior mode based on FEMA 306

Wall	Pier	h_{eff} (mm)	V_r (kN)	V_{bsj1} (kN)	V_{bsj2} (kN)	V_{dt} (kN)	V_{tc} (kN)
West	Door	1842	6.08	39.8	7.05	24.5	6.73
	Central	1335	24.6	65.2	12.95	59.8	27.3
	Window	1469	3.97	27.0	5.6	16.6	4.34
East	Door	2043	5.48	39.8	7.05	24.5	6.03
	Central	1278	25.7	65.2	12.95	59.8	28.3
	Window	1546	3.77	27.0	5.6	16.6	4.12

wall, respectively) were used and the walls are treated as primary elements. The idealized non-linear force-deflection is plotted against the hysteretic response of the west wall and east wall in Fig. 7(a) and (b), respectively. As shown here and noted in FEMA 307 (FEMA [14]), the experimentally obtained displacements that occurred under a stable rocking mechanism exceed the proposed drift value for collapse for primary elements, as specified in FEMA 273. Furthermore, as also noted in FEMA 307 and observed here, the rocking capacity does not drop to a value of 60% of the initial capacity as proposed by FEMA 273. Finally, FEMA 307 comments that a sequence of different behaviors is common in experiments. The rocking shifting to bed-joint sliding for the central pier, observed when pushing the building in the south direction, is consistent with this expectation.

After this first series of tests, it was observed that the diaphragm remained elastic throughout the tests, as shown in Fig. 9. Therefore, to force the diaphragm into the inelastic range and to investigate the effectiveness of a repair procedure, it was decided to reinforce the shear walls with fiberglass materials.

3. Repair

The shear walls were repaired using Tyfo fiberglass strips as shown in Fig. 10. Note that these strips are frequently used to enhance the out-of-plane performance of unreinforced masonry walls (Tyfo Systems [15]). No back pointing, grout or epoxy injections were used to repair the cracks in the wall, only fiberglass materials was used. The in-plane rocking behavior of unreinforced masonry walls is generally perceived as a stable desirable behavior, but there may be instances where the available rocking strength of such walls may still be inadequate. In that perspective, Tyfo strips were applied to the shear walls to increase their in-plane capacity. They were designed to increase the rocking force capacity of each pier, but

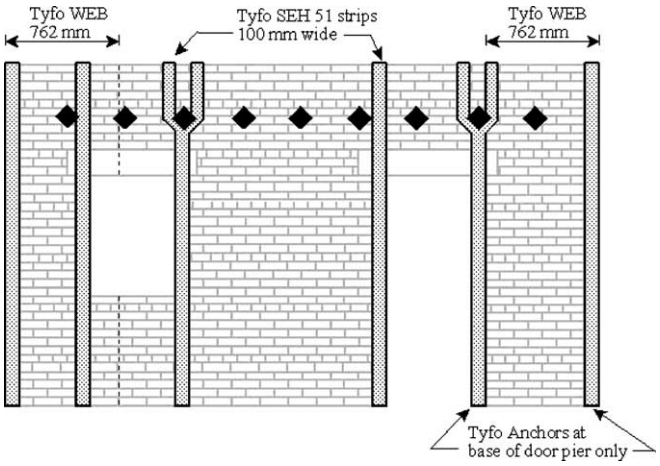

Fig. 10. West wall elevation of URM specimen repaired with Tyfo strips and web (the east wall is simply a mirror image).

to keep that rocking capacity below the pier shear capacity. Hence, the objective of this repair strategy is to use the Tyfo strips to preserve the desirable pier rocking mode, increase capacity and enhance the displacement ductility of the repaired shear walls. The corners of the continuous and discontinuous walls were wrapped with Tyfo WEB to increase their shear resistance. This fabric not only provides additional shear strength, but also maintains the wall's integrity by preventing spalled portions of the wall from breaking off and becoming safety hazards.

The specimen was re-tested with the same input motion as before. During La Malbaie × 0.5 and × 1.0 pseudo-dynamic tests, the displacements of both east and west shear walls were considerably reduced while maintaining the same level of force as recorded for the original specimen. With the increasing ground motion, during La Malbaie × 1.5 and × 2.0, the wall response was characterized by larger forces and reduced lateral displacements as compared to the original specimen. Hysteretic force–displacement curves for the repaired and original specimen during La Malbaie × 2.0 run are shown in Fig. 11(a) and (b). It can be observed that the lateral forces in the east and west wall were increased by approximately 48% as compared with the original specimen, whereas the corresponding displacements were considerably reduced. As a result of the increased stiffness of the repaired piers, the rocking motion was significantly reduced, as shown in Fig. 8. The specimen was then subjected to La Malbaie × 3.0 test run, resulting in the development of new cracks in the walls and localized debonding of Tyfo material. Additional cracks were formed near the concrete foundation below the central pier on the west wall. As the level of excitation was increased, some strips started to de-bond, yet still providing enough deformation capacity to allow rocking as shown in Fig. 12 (note a visible 10 mm wide crack opening). However, for the central pier demonstrating a bed-joint sliding behavior, the Tyfo strips were mainly subjected to shear stresses and ultimately failed in shear by tearing, as shown in Fig. 13. Some tearing was also observed in the Tyfo WEB overlay at the corners due to out-of-plane tensile cracks. Finally, the specimen was subjected to La Malbaie × 4.0. Additional de-bonding and tearing of the Tyfo material (strips and web) were observed and more extensive cracking developed in the walls. The repeated rocking and sliding behavior of the piers induced tears and de-bonding, limiting the wall capacity to approximately 66 kN, resulting in increased lateral displacements.

Finally, as shown in Fig. 14, the specimen was subjected to more conventional cyclic-testing, by increasing center-span displacement until a large proportion of the Tyfo material (strips and web) was almost completely de-bonded from the shear wall surface. Because of the existing crack pattern, repointing prior to the repair would not have improved the observed behavior. However, a different behavior could have been observed in a retrofit perspective

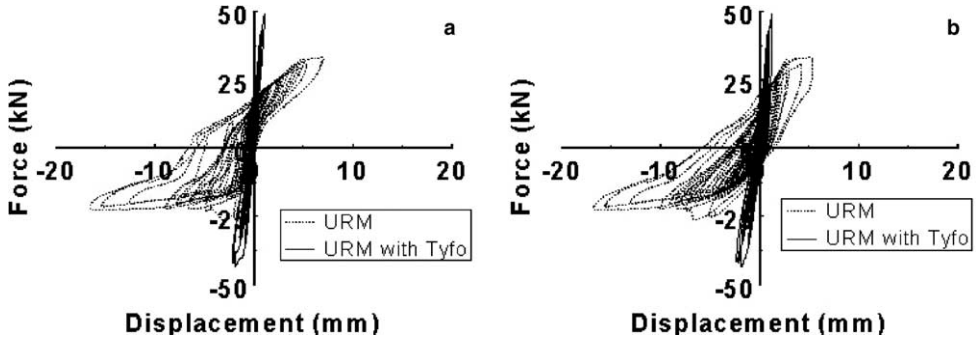

Fig. 11. Hysteretic response of URM during La Malbaie × 2.0 before and after Tyfo repair: (a) west wall; (b) east wall.

Fig. 12. Pier rocking at base of central pier with Tyfo repair during La Malbaie × 4.0.

Fig. 13. Tyfo strip failed in shear.

because the original structure would not have been pre-cracked prior to application of the fiberglass material.

Strengthening the shear walls with Tyfo materials did increase the force on the diaphragm, as shown in Fig. 15, where some non-linear diaphragm behavior initiated during La Malbaie × 4.0.

4. Evaluation of wood diaphragm response

4.1. Models and theoretical values

The dynamic response of the wood diaphragm was also investigated. It is addressed specifically in various documents such as the UCBC (ICBO [1]), FEMA 178 (FEMA [3]), the CGSEEB (NRC [11]), and the Prestandard and Commentary for the Seismic Rehabilitation of Buildings (FEMA 356) (FEMA [16]). In the CGSEEB, FEMA 178, and the UCBC 1997, the dynamic response is essentially assessed by calculating a normalized demand-capacity ratio (DCR). For the special evaluation methodology to be applicable, any given point defined by the DCR and the span, L, must fall within the boundaries of the graph in Fig. 16. This figure has been developed to control the severity of the diaphragm displacements and velocities at mid-span. It also ensures that the horizontal deflection of the diaphragm does not produce instability of the out-of-plane walls by providing limits on slenderness ratios derived from dynamic stability concepts. For the tested specimen, the DCR is 1.05, and given the diaphragm span of 5.28 m, it is confirmed that the point (1.05, 5.28) falls in region 3 of Fig. 16.

FEMA 356 defines the capacity of a diaphragm by its yield shear capacity. The elastic maximum deflection of a wood diaphragm is given by

$$\Delta = \frac{v_y L}{2G_d}, \tag{1}$$

where v is the shear at yield in the direction under consideration, L is the diaphragm's span, and G_d is the diaphragm shear stiffness taken as 3152 kN/m (18,000 lb/in) and 1576 kN/m (9000 lb/in) for chorded and unchorded diagonal sheathing with straight sheathing, respectively (FEMA [16]).

The non-linear inelastic deformation of the diaphragm is determined by a generalized force-deformation relation defined by parameters d, e, and c, as shown in Fig. 17, where d is the maximum deflection at the point of first loss of strength taken as 1.5 times the yield strength, and e is the maximum deflection at a reduced strength c.

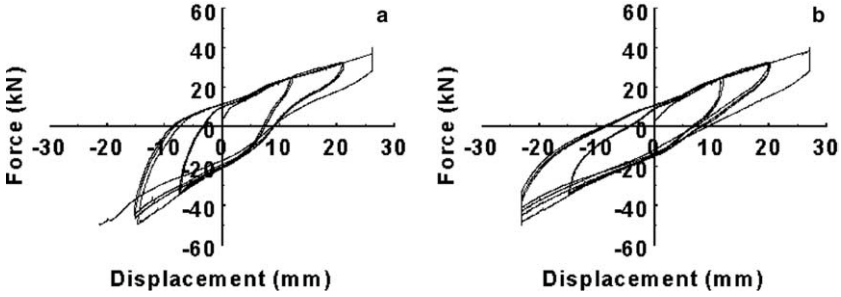

Fig. 14. Hysteretic response during cyclic test: (a) west wall; (b) east wall.

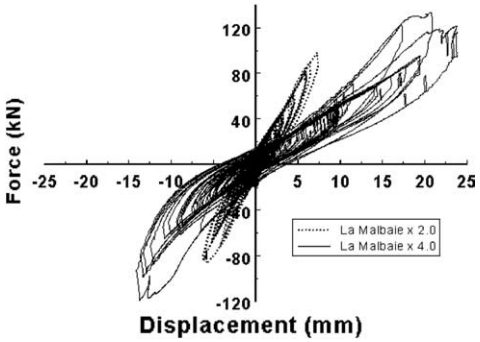

Fig. 15. Comparison of diaphragm center-span hysteretic response with shear wall repaired with Tyfo material during La Malbaie × 2.0 and × 4.0.

Alternatively, the ABK methodology (ABK [17]) expresses force-deformation envelopes for different type of wood diaphragms by a second-order curve defined by:

$$F(e) = \frac{F_u e}{\frac{F_u}{k_i} + e}, \tag{2}$$

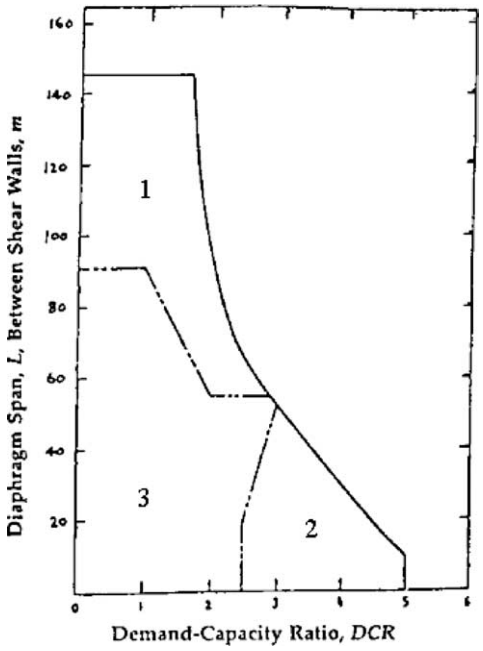

Fig. 16. Acceptable diaphragm span versus demand-capacity ratio (DCR) (NRC 1992).

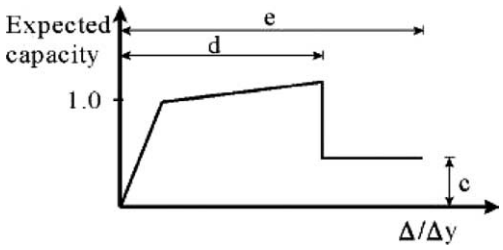

Fig. 17. FEMA 356 generalized force-deformation relation for wood diaphragm.

where $F(e)$ is the force at the diaphragm's end, e is the mid-span deformation, k_i is the initial stiffness, and F_u is the ultimate force (asymptote). The ultimate force, F_u, is given by the unit shear strength of the diaphragm, v_u, multiplied by its width, D.

4.2. Comparison with experimental results

Using the data recorded by the three temposonics located across the span of the diaphragm as well as the LVDTs on each shear wall, the lateral force-deformation relationship of the diaphragm was investigated. The hysteretic response of the wood diaphragm during La Malbaie × 2.0 is shown in Fig. 18, and is essentially linearly elastic. The maximum floor deformation (center relative to ends) recorded at mid-span was 5.54 mm under a 66.5 kN force. Using Eq. (1) from FEMA 356, the calcu-

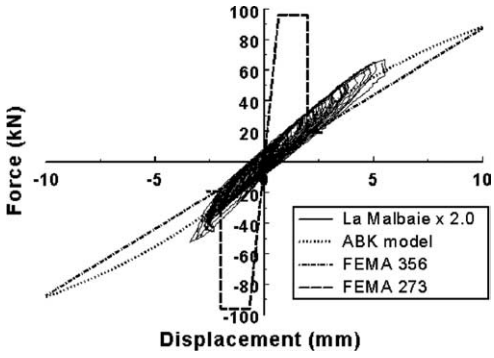

Fig. 18. Comparison of hysteretic response of wood diaphragm during La Malbaie × 2.0 with FEMA 356, FEMA 273 and ABK force-deformation relations.

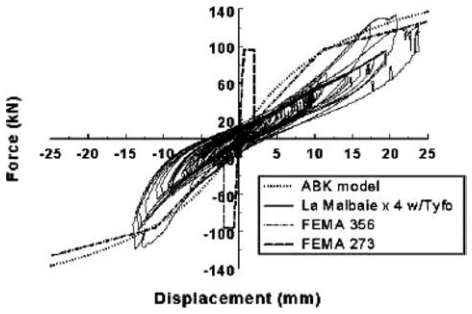

Fig. 19. Hysteretic response of wood diaphragm with shear walls repaired with Tyfo for La Malbaie × 4.0, with FEMA 356, FEMA 273 and ABK force-deformation relations.

lated mid-span deflection is 7.61 mm for chorded diaphragm. For the sake of comparison, FEMA 273 which uses a slightly different equation is also included in Fig. 18.

Using the force-deformation envelope from ABK, Eq. (2), and rearranging the terms, the calculated deflection is 6.45 mm, for a force of 33.25 kN (i.e., 66.5/2 kN) at the end of the diaphragm, which also matches closely the experimentally obtained deflection.

The in-plane lateral load-resisting capacity of the repaired shear walls was increased as compared to the original walls. As a result, larger forces were developed, thus inducing larger relative displacements between the diaphragm and shear walls. As observed in Fig. 19, a maximum mid-span deflection of 23.9 mm was recorded under a load of 115.8 kN for La Malbaie × 4.0. Corresponding deformations under such load is 16.6 mm for the ABK model, and 20.0 mm for chorded diaphragm using the force-deformation relation from FEMA 356. Again, both FEMA 356 and ABK give diaphragm deflections relatively close to those obtained experimentally. Experimental results for the diaphragm closely follow the FEMA 356 and ABK models in the linear elastic range, but since the diaphragm did not undergo very large inelastic deformations, it is not known whether it would behave as predicted by both models up to its ultimate. For the sake of comparison, FEMA 273 which uses a slightly different equation is also included in Fig. 19. After the test, examination showed that, contrary to pre-test calculations that predicted otherwise, the diaphragm remained relatively intact. Damage was limited to some popped out nails at each ends of the diaphragm.

5. Conclusions

A full-scale one-story unreinforced brick masonry specimen having a flexible wood diaphragm was tested pseudo-dynamically. Tests results have shown that stable combined rocking and sliding mechanisms formed and large deformations developed without significant strength degradation. The diaphragm remained, however, essentially elastic throughout. The difference in wall response due to the presence of continuous or discontinuous corners was somehow negligible during high intensity seismic excitation producing inelastic wall response. The specimen was repaired using Tyfo fiberglass strips, which increased the lateral strength of the shear wall while significantly reducing the displacements. The theoretical seismic response was calculated using different codified evaluation methodologies.

It was found that some (but not all) of the existing procedures accurately capture the rocking sliding behavior that developed in the shear walls under large displacement. The FEMA 306 procedure proved the most accurate for evaluation purpose while other missed one or more points of behavior. Although not tested to its ultimate capacity, the diaphragm deflections observed experimentally closely matched those predicted using the FEMA 356 and ABK models.

The dynamic response of existing unreinforced masonry buildings should be further investigated. Notably, additional studies should investigate the effect of the non-linear response of diaphragms with different types of lumber sheathing arrangements, and diaphragm rehabilitated with plywood sheathing.

Acknowledgments

The authors acknowledge the financial support provided by the Natural Science and Engineering Research Council of Canada (NSERC), Brampton Brick, Fitzgerald Building Supplies (1996) Limited, Ottawa Region Masonry Contractors Association, International Union of Brick Layers and Allied Craftsmen (Industrial Promotion Fund), Canadian Portland Cement Association, George and Asmussen Limited, R.J. Watson Inc., Fyfe Co. L.L.C. Contributions by Dr. Svetlana Nikolic-Brzev from the British Columbia Institute of Technology are also appreciated.

References

[1] ICBO. Uniform code for building conservation. Whittier (CA): International Conference of Building Officials; 1997.
[2] ABK, A Joint Venture, Methodology for mitigation of seismic hazards in existing unreinforced masonry buildings: the methodology. Rep. ABK-TR-08, Agbabian & Associates, S.B. Barnes & Associates, and Kariotis & Associates, El Segundo, CA, 1984.
[3] FEMA 178. NEHRP handbook for the seismic evaluation of existing buildings. Washington (DC): Building Seismic Safety Council; 1992.
[4] Bruneau M. Seismic evaluation of unreinforced masonry buildings – a state-of-the-art report. Can J Civ Eng, Ottawa, Canada 1994;21(3): 512–39.
[5] Bruneau M. State-of-the-art report on the seismic performance of unreinforced masonry buildings. J Struct Eng, ASCE 1994;120(1): 230–51.
[6] Bruneau M. Preliminary report of structural damage from the Loma Prieta (San Francisco) earthquake of 1989 and pertinence to Canadian structural engineering practice. Can J Civ Eng, Ottawa, Canada 1990;17(2):198–208.
[7] Bruneau M. Performance of masonry structures during the 1994, Northridge (L.A.) earthquake. Can J Civ Eng, Ottawa, Canada 1995;22(2):378–402.

[8] Rutherford and Chekene. Damage to unreinforced masonry buildings in the Loma Prieta earthquake of October 17, 1989. Sacramento, USA: California Seismic Safety Commission; 1991. 38p.
[9] Costley AC, Abrams DP. Dynamic response of unreinforced masonry buildings with flexible diaphragms. Rep. No. UILU-ENG-95-2009, Department of Civil Engineering. University of Illinois at Urbana-Champaign, Urbana, Ill., 1995.
[10] Paquette J, Bruneau M. Seismic testing of unreinforced masonry building with flexible diaphragm. Ottawa Carleton Earthquake Engineering Research Centre, Rep. No. OCEERC-02-25, Ottawa, 2002.
[11] NRC. Guidelines for seismic evaluation of existing buildings. Ottawa, Canada: Institute for Research in Construction, National Research Council; 1992.
[12] FEMA 273. NEHRP guidelines for the seismic rehabilitation of buildings. Washington (DC): Building Seismic Safety Council; 1997.
[13] FEMA 306. Evaluation of earthquake damaged concrete and masonry wall buildings, basic procedures manual. Washington (DC): The Patnership for Response and Recovery; 1999.
[14] FEMA 307. Evaluation of earthquake damaged concrete and masonry wall buildings, technical resources. Washington (DC): The Patnership for Response and Recovery; 1999.
[15] Tyfo Systems. For unreinforced masonry (URM) and reinforced concrete/masonry wall strengthening. San Diego (CA): Fyfe Co. L.L.C.; 1997.
[16] FEMA 356. Prestandard and Commentary for the Seismic Rehabilitation of Buildings. Washington (DC): Federal Emergency Management Agency; 2000.
[17] ABK, A Joint Venture, Methodology for mitigation of seismic hazards in existing unreinforced masonry buildings: Interpretation of diaphragm tests. Rep. ABK-TR-05, Agbabian & Associates, S.B. Barnes & Associates, and Kariotis & Associates, El Segundo, CA., 1982.